



# SURFACE MORPHOLOGY STUDY IN LASER PAINT REMOVAL MECHANISMS ON SELECTED NATIONAL CAR COATED SUBSTRATE

Mohammad Khairul Azhar Abdul Razab<sup>1</sup>, Mohammad Suhaimi Jaafar<sup>2</sup>, Nor Hakim Abdullah<sup>1</sup>, Mohamad Faiz Mohd Amin<sup>1</sup> and Mazlan Mohamed<sup>1</sup>

<sup>1</sup>Advanced Materials Research Cluster, Faculty of Earth Science, Universiti Malaysia Kelantan, Jeli, Kelantan, Malaysia

<sup>2</sup>School of Physics, Universiti Sains Malaysia, Minden, Penang, Malaysia

E-Mail: [azhar@umk.edu.my](mailto:azhar@umk.edu.my)

## ABSTRACT

Thirty six rectangular shapes of two type's national car coated substrate samples were irradiated by using Nd: YAG laser for paint removal. The best and worst crater depth of highest laser paint removal efficiency was selected for surface morphology analysis by using Nova NanoSEM 450. The results show the surface texture of the crater depth was changed and varies based on the paint residue left after the paint stripping process.

**Keywords:** laser, FESEM, paint removal, thermal decomposition, national car.

## 1. INTRODUCTION

Current studies show that laser cleaning can be a good alternative candidate to replace conventional chemical cleaning in paint removal purposes which consume much water and cost [1-6]. This new cleaning methods also has advantages in absence of mechanical damage of the metal surface and at the same time increase the effectiveness of paint removal [5, 7].

Paint removal mechanism begins after the absorption of laser intensity to the paint layers exceeds the ablation threshold of the material [8-12]. The average coating removal efficiency ( $\epsilon$ ) in laser paint removal is depending on the painted composition itself as well as the appropriate laser parameters have been used [4, 13]. Nevertheless, the information of irradiated surface morphology and its relations to  $\epsilon$  as well as laser parameters are still not well documented due to lack of research studies have been done [14]. Thus, this study aimed to investigate the surface morphology and factors influenced the texture and structured pattern of irradiated crater depth over two types of national car coated substrates.

## 2. METHODOLOGY

### Operation procedure

Thirty six rectangular shapes of car coated substrate samples were acquired from two types of national car models A and B with the coating system were orange metallic acrylic and black metallic acrylic and never repaints. The paint thickness was determined by using CEM DT-156 Paint Coating Thickness Gauge Tester F/NF Probe and ranged from 92-134  $\mu\text{m}$  and 196-450  $\mu\text{m}$  for substrate samples A and B respectively.

Each type of substrate sample A and B was marked by unique numbers from 1 to 18 for ten laser irradiations by using Nd: YAG laser. The laser fluence, F was increased with 10 J/cm<sup>2</sup> for each shoot and pulse width (PW), repetition rate (RR) and beam size (BS) were manipulated as listed in the Table-1. The experiment was carried out in the Medical Physics Laboratory, School of

Physics, University Sains Malaysia, Penang and Material Science Laboratory, Faculty of Earth Science, University Malaysia Kelantan Jeli Campus.

Irradiated sample was cleaned by using plain water and dried to remove any burning residue existed. Tissue paper was used to swap the stripped area in order to ensure there were no more residues of paint flakes left. More important, the originality of the structure, pattern, contour and texture of the irradiated crater depth were sustained from any physical and chemical distortion before proceed to Field Emission Scanning Electron Microscopy (FESEM) analysis.

### Determination of paint removal efficiency

Paint removal efficiency generally is the function of laser parameters including beam intensity, PW, RR and BS of the irradiation spot area. For coating removal by laser irradiation, the efficiency of the process can be defined by using Eqn. (1) [15, 16].

$$\epsilon = V / E = d / nF \quad (1)$$

where  $\epsilon$  is the average coating removal efficiency ( $\mu\text{m cm}^2 \text{ J}^{-1}$ ), V is the volume of coating removed and E is the total laser energy, d is the depth of coating removed, F is the laser fluence and n is the number of laser shoots.

The removal depths (d) over the incident laser fluence (F) were plotted for each PW, RR and BS. Hence, the  $\epsilon$  of each laser parameters applied on a certain sample determined by measuring their inclination slope of each fitted linear graph.

### Substrate sample selection

Surface morphology was investigated on a selected crater depth considered from the selected substrate sample of higher and lower  $\epsilon$  as shown in Table-2. Meanwhile, non-irradiated area was selected randomly from each two type of non-selected substrate samples as a control for this analysis. Nova NanoSEM 450 manufactured by FEI Company, USA was used to perform FESEM analysis on the selected crater depth as shown in Figure-1.

**Table-1.** Laser parameters considered for 3 mm and 5 mm BS with varies in F, PW and RR.

Sample Number	Number of Irradiation	BS (mm)	F (J/cm <sup>2</sup> )	PW (ms)	RR (Hz)
1	10	3	210-300	100	1.0
2	10	3	210-300	200	1.0
3	10	3	210-300	300	1.0
4	10	3	210-300	100	1.5
5	10	3	210-300	200	1.5
6	10	3	210-300	300	1.5
7	10	3	210-300	100	2.0
8	10	3	210-300	200	2.0
9	10	3	210-300	300	2.0
10	10	5	150-240	100	1.0
11	10	5	150-240	200	1.0
12	10	5	150-240	300	1.0
13	10	5	150-240	100	1.5
14	10	5	150-240	200	1.5
15	10	5	150-240	300	1.5
16	10	5	60-150	100	2.0
17	10	5	60-150	200	2.0
18	10	5	60-150	300	2.0

Note: Maximum F for 3 mm BS is 300 J/cm<sup>2</sup> for all laser parameters. Meanwhile, the maximum F for 5 mm BS is 240 J/cm<sup>2</sup> set-up with RR 1.0 and 1.5 Hz, whereas 150 J/cm<sup>2</sup> set-up with RR 2.0 Hz.

**Table-2.** Selected crater depths from highest and lowest  $\epsilon$  of substrate samples A, B and C.

Substrate Sample	Selected Substrate Sample	Selected Crater Depth
A	A 10	Number 7
	A 5	Number 2
	Non-irradiated sample A	-
B	B 11	Number 3
	B 4	Number 4
	Non-irradiated sample B	-

depth surface to produce different types of electron emissions. A detector was caught secondary electrons produced and an image of the crater depth surface was constructed by comparing the intensity of these secondary electrons to the scanning primary electron beam. A location of the selected crater depth was then navigated for required region of interest (ROI) scanning. Finally, high resolutions of the scanned ROI was appeared on the display monitor ranged from 1000-100, 000  $\mu\text{m}$ , represented the selected crater surface morphology. This process was repeated for the next selected substrate samples.

### FESEM analysis

Before proceed to FESEM analysis, the selected crater depth was coated with Platinum (Pt) by using JEOL JFC-1600 Auto Fine Coater in order to enhance the resolutions of the scanning micrograph obtained. The coating thickness was set-up for 10 nm with 40 s sputtering time and 30 mm source to target distance of the Pt source to the crater target.

The selected substrate sample was then prepared for FESEM analysis by attaching to the provided sample stand by using adhesive tape as shown in Figure-2. A stand was suited at the center of provided slot into the vacuum chamber prior 5 mm source to target distance of the electron gun to the substrate sample was set-up. Gun pressure was then pumped air chamber to a certain pressure and provides a vacuum space in the chamber cavity. This condition was enabled the electrons to be generated by a field emission source which leads to electron acceleration in a field gradient.

The electron beams then passed through the electromagnetic lenses and bombards the selected crater

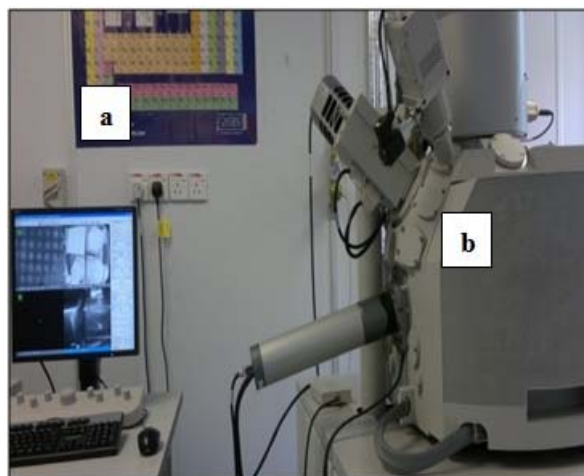


**Figure-1.** Nova NanoSEM 450 and to perform surface morphology analysis of the targeted ROI (a) Computer unit for image morphology analysis (b) NanoSEM 450 chamber.



**Figure-2.** Substrate sample tightly attached and fixed to the sample stand for electron beam bombardment by using an electron gun in the vacuum chamber (a) Substrate sample.

### 3. RESULTS AND DISCUSSION

#### Surface morphology analysis onto selected crater depth

The surface morphology of best and worst of selected crater depths from sample A and B were analyzed by using Nova NanoSEM 450 on the selected ROI as shown in Figures-3-6. In addition, non-irradiated ROI was selected randomly from each two type of substrate samples and becomes a control for its corresponding samples A and B as shown in Figures-7 and 8.

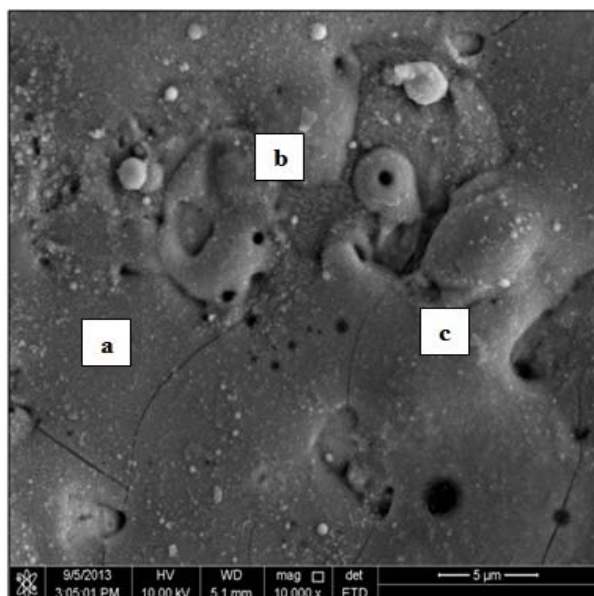


**Figure-3.** Surface morphology for pulse width 100 ms, repetition rate 1.0 Hz, beam size 5 mm and fluence energy 180 J/cm<sup>2</sup> for sample A10 (a) Precipitate subtle line obtained on the ROI selected represents the fine cracks on the irradiated surface (b) A few of small holes clearly seen on the crater surface (c) Surface morphology was uniform in term of its texture and structure pattern.

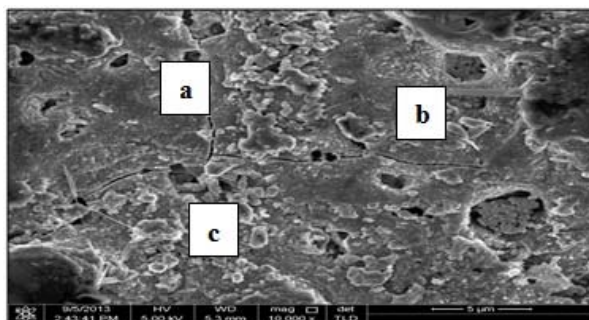


**Figure-4.** Surface morphology for pulse width 200 ms, repetition rate 1.5 Hz, beam size 3 mm and fluence energy 290 J/cm<sup>2</sup> for sample A5 (a) Precipitate coarse line obtained on the ROI selected represents the serious cracks on the irradiated surface (b) Most of big and small holes clearly seen on the crater surface (c) Grain surface morphology with minor epitaxial growth randomly spread out leads to non-uniform surface texture and structure pattern.

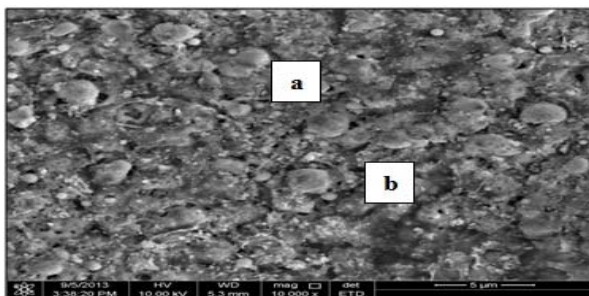


**Figure-5.** Surface morphology for pulse width 200 ms, repetition rate 1.0 Hz, beam size 5 mm and fluence energy 220 J/cm<sup>2</sup> for sample B11 (a) Minor grains spherical shape clearly seen on the ROI selected (b) Many of small holes detected around the irradiated surface.

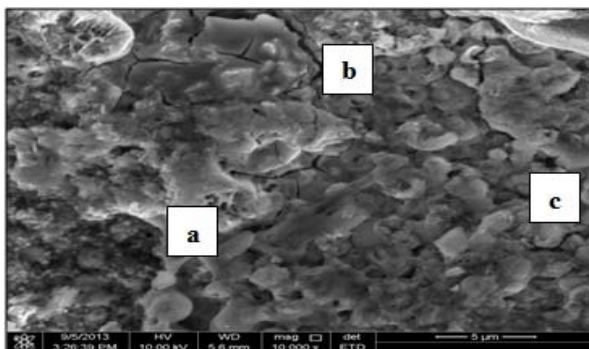


**Figure-6.** Surface morphology for pulse width 100 ms, repetition rate 1.5 Hz, beam size 3 mm and fluence energy 270 J/cm<sup>2</sup> for sample B4 (a) Major grains amorphous shape clearly seen on the ROI selected (b) Precipitate coarse line detected on the ROI selected represents the major cracks on the irradiated surface (c) Many of small holes obtained around the selected ROI leads to non-uniform on the irradiated surface.



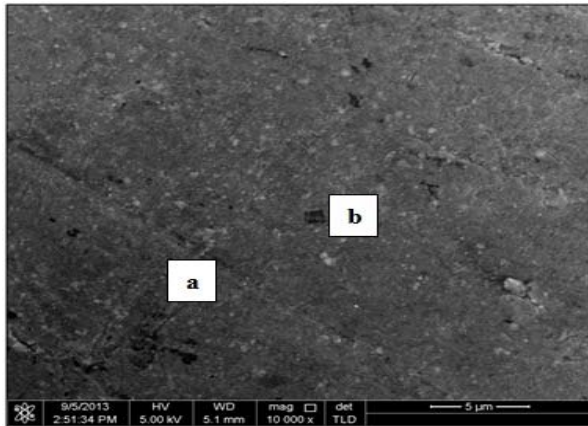


**Figure-7.** Surface morphology for non-irradiated ROI of sample A (a) Subtle line defects on the top coat surface (b) Small hole existed on the uniform top coat surface detected.

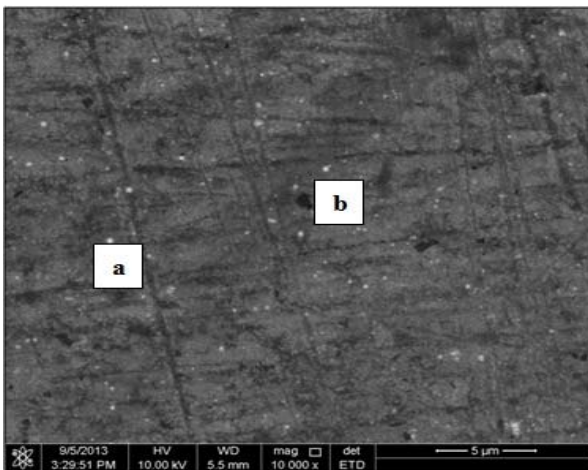


**Figure-8.** Surface morphology for non-irradiated ROI of sample B (a) A few of subtle lines defects detected on the surface (b) Small hole existed on the uniform surface clearly seen.

#### Factor affects the surface texture of crater depth

Properties of the surface morphology are depending on the efficiency of thermal decomposition process occurred on paint layers either the paint layers are uniformly removed or paint residues are still existed after irradiation process [14]. From the results, a few defects on the crater depth surface are detected from selected samples A and B sort of cracking, fine and coarse lines, grains spherical surface, amorphous carbon shapes of the crater surface and many more. These defects are mainly due to thermal induced which resulted from the thermal decomposition mechanism during the paint removal process [1, 14, 17].

Paint removal is considered almost complete for best selected crater depth of sample A as shown in Figure-3, where only a few of precipitate subtle lines were obtained. However, the thermal decomposition process

was not completely done for worst selected crater depth of sample A, where a few of coarse lines were detected to obtain serious cracks on the crater surface as shown in Figure-4. Moreover, it was clearly seen the minor epitaxial growth was randomly spread out on the worst selected crater surface due to paint re-solidification after the stripping process.

For sample B, the best selected crater depth produced minor grains spherical shape and a few of small holes were detected around the crater surface as shown in Figure-5. This indicates the paint material was not uniformly removed and minor roughened the surface texture. Meanwhile, the worst selected crater depth of sample B produced a lot of major grain amorphous shape which indicates the paint residue was not completely removed but re-solidified on the irradiated area. Furthermore, a few of coarse lines were detected around the crater surface which leads to serious cracks as shown in Figure-6.

#### 4. CONCLUSIONS

It is shown the surface texture of the crater depth was changed and varies based on the paint residue left after the paint stripping process. Thus, the morphology surface was also effected where a few of defects detected by using FESEM analysis sort of coarse and subtle lines, cracks and non-uniformity of the irradiated surface as shown in Figures-3-6. This condition was dependent on the thermal effects which resulted to paint the material melting and carbonization obtained which leads to roughen the crater surface [1]. The results also conclude the sample A have higher efficiency in laser paint removal mechanisms than sample B in term of surface texture and structure pattern uniformity.

#### ACKNOWLEDGEMENT

The authors acknowledge the support of the Short Term Research Grant Scheme [Grant Number R/SGJP/A08.00/00451A/001/2015/000241] awarded by University Malaysia Kelantan. Appreciation also goes to Mr. Yahya Ibrahim and Mrs. Ee Bee Choo of the School of Physics University Sains Malaysia and Mr. Ahmad Fadli Ahmad Sanusi of the Faculty of Earth Science, University Malaysia Kelantan Jeli Campus for their help in preparing the laser equipment and its accessories during the experiments and FESEM analysis. Many thanks also go to Miss Illya Syazwanie Ahmad Mazalan as a data accumulator for this research project.

#### REFERENCES

- [1] G. X. Chen, T. J. Kwee, K. P. Tan, Y. S. Choo and M. H. Hong. 2010. Laser cleaning of steel for paint removal. *Applied Physics A*. 101(2): 249-253.
- [2] Steen W. M. and Mazumder J. 2010. *Laser material processing*. 4<sup>th</sup> Ed. Springer. Berlin, Germany.



- [3] M. K. A. A. Razab, M. S. Jaafar, A. A. Rahman and S. A. Saidi. 2014. Determination of average coating removal efficiency for Nd: YAG laser over three types of car coated substrate. *Advances in Environmental Biology*. 8(1): 227-236.
- [4] M. K. A. A. Razab, M. S. Jaafar and A. A. Rahman. 2014. A study of temperature effects on car coated substrate in laser paint removal. *International Journal of Engineering & Technology*. 14(2): 39-48.
- [5] M. K. A. A. Razab, M. S. Jaafar, A. A. Rahman, S. Mamat and M. I. Ahmad. 2014. Study of health implications effects in laser paint removal process based on PM1.0 and PM10.0 measurements. *Journal of Tropical Resources and Sustainable Science*. 2(1): 30-39.
- [6] M. K. A. A. Razab, M. S. Jaafar and A. A. Rahman. 2014. A study of particulate matter concentration released during laser paint removal process on car coated substrate. *IOSR Journal of Applied Physics*. 2014. 6(2): 40-48.
- [7] Veiko V. P., Mutin T. J., Smirnov V. N., Shakhno E. A. and Batishche, S. A. 2008. Laser cleaning of metal surfaces: Physical processes and applications. In: *Fundamentals of Laser Assisted Micro-and Nanotechnologies*. pp. 1-8.
- [8] Poprawe, R. 2011. *Tailored light 2: Laser application technology*. Springer. Berlin, Germany.
- [9] Targowski P., Ostrowski, R., Marczak J., Sylwestrzak M. and Kwiatkowska E. A. 2009. Picosecond laser ablation system with process control by Optical Coherence Tomography. In: *SPIE Europe Optical Metrology*. pp. 1-8.
- [10] M. K. A. Abdul Razab, M. S. Jaafar, A. A. Rahman and S. A. Saidi. 2014. Estimation of threshold fluence, absorption coefficient and thermal loading of car coated substrate in laser paint removal. *Applied Mechanics and Materials*. 554: 439-443.
- [11] Razab, M. K. A. A., Jaafar, M. S., Rahman, A. A., Mamat, S., Ahmad, M. I., & Suhaimi, F. M. 2015. Influenced of threshold fluence, absorption coefficient and thermal loading in laser paint removal mechanisms. In: *Environment, Energy and Applied Technology*. W. P. Sung and J. C. Kao (Eds.). pp. 885-891.
- [12] Mongelli G. 2005. Portable handheld laser small area supplemental coatings removal system. [http://db.materialoptions.com/ASETSDDefense/SEDB/CrPrimer\\_VOC\\_Alts/Tech\\_Matls\\_Info/Handheld%20laser%20paint%20stripping.pdf](http://db.materialoptions.com/ASETSDDefense/SEDB/CrPrimer_VOC_Alts/Tech_Matls_Info/Handheld%20laser%20paint%20stripping.pdf).
- [13] Koh Y. and Sarady I. 2001. Removal of adhesives and coatings on iron artifacts using pulsed TEA CO<sub>2</sub> and Nd: YAG lasers. In: *Lasers in Metrology and Art Conservation*. pp. 46-53.
- [14] M. K. A. A. Razab, M. S. Jaafar, A. A. Rahman and S. A. Saidi. 2014. Identification of optimum operatives parameters for Pulse Nd: YAG laser in paint removal on different types of car coated substrate. *International Journal of Education and Research*. 2(2): 47-64.
- [15] D. E. Roberts. 2004. Pulsed laser coating removal by detachment and ejection. *Applied Physics A*. 79(4-6): 1067-1070.
- [16] X. Zhou, K. Imasaki, H. Furukawa, H. Umino, K. Sakagishi, S. Nakai and C. Yamanaka. 2001. A study of the surface products on zinc-coated steel during laser ablation cleaning. *Surface and Coatings Technology*. 137(2): 170-174.
- [17] Labuschagne K. and Pityana S. L. Laser induced damage threshold on metallic surfaces during laser cleaning. In: *3<sup>rd</sup> International WLT-Conference on Lasers in Manufacturing*. pp. 1-5.